Interaction Region Optimization for CESR Phase III

James J. Welch

Cornell University, Ithaca, NY 14853 *

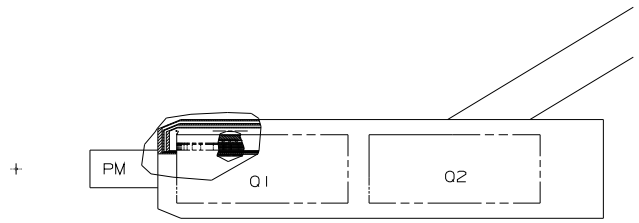

Figure 1: A sketch of the superconducting IR magnets for CESR phase III.

Introduction

The space around the interaction region is some of the most highly utilized due to its importance to both CESR and CLEO. It is therefore desirable to try to optimize the design of the components in that space to a greater extent than is usually done for accelerator systems.

In this paper I describe an optimization of the CESR portion of interaction region I developed and used to generate the specifications for the superconducting magnets for the phase III interaction region. The superconducting magnet design grew from an idea for B factory IR magnets which was discussed as early as the Syracuse workshop in 1989 [1]. It was given a permanent magnet nose and developed for an equal energy configuration by the IR Task Force group starting in 1991 and integrated with the design of CLEO III [2]. The most recent design, and the one on which this based, was developed by D. Rice and E. Nordberg in 1994, [3]. They incorporated a superconducting horizontally focussing quadrupole in the same cryostat as the vertically focussing quadrupole, thus greatly reducing the overall focal length of the IR magnets and enhancing the capacity to create round beam focal spots. One assembly of superconducting IR magnets, as specified in a recent RFP for their construction, is shown in figure 1.

The goal of the optimization was to maximize the luminosity by varying a number of design parameters such as the bore diameter, length and positions of the superconducting magnets. The optimization was unusual in that it had a wide mix of constraints and types of dependencies. I took into account mechanical constraints and relationships, beam stayclear criteria, magnet design limitations (both permanent and superconducting), lattice matching constraints, pretzel matching conditions, synchrotron radiation constraints, and various head-on and long-range beam-beam effects. In the design of the interaction region one frequently faces questions such as: How much luminosity is lost or gained for a one centimeter change in the detector stayclear? With the optimization program I tried to answer some such questions in a meaningful way.

A major complication was the need to simultaneously optimize collision and injection conditions. Injection by itself is rather complicated as there are four different beamlines to consider. During collision only two beamlines have to be generated, one for incoming beams and one for outgoing beams; outgoing electron and positron trajectories are identical. However, during injection, no two beamlines are the same and each has to be calculated to determine aperture and long-range beam-beam effects. So in all, to optimize the interaction region six closed orbits have to be generated and simultaneously varied. The beta functions are not different between injection and collision, only the closed orbits differ.

A related complication was the difference in constraints between injection and collision. During injection one can relax the radiation requirements somewhat because the detector is not taking data so the deadtime generated is irrelevant. Furthermore the lifetime of the beam need not be as good as injection doesn't take as long as collision, so more long-range interaction can be tolerated. Relaxing the injection parameters proved to be crucial to finding a solution that was not entirely limited by its performance during injection.

The same program and constraints will be used in the near future to help determine the final specifications for the permanent magnet quadrupoles just in front of the superconducting magnets. In principle, the optimization program should be useful in understanding the behavior of the beam in the phase II lattice as well, particularly during injection. It also serves as a convenient vehicle to keep track of the numerous design parameters that are interdependent and frequently change. Many of these are listed in the Appendix.

*Work supported by the National Science Foundation

General Procedures and Assumptions

The optimization centered around the flat beam phase III design for 5.289 GeV. For round beam optics the required gradients for Q1 and Q2 are less than that required for Q1 in the flat beam case. Both round and flat optics want shorter, stronger, closer quadrupoles. There may be some difference in the optimization of the bore diameter between the round and flat; this was not studied.

The distribution of bunches was assumed to be nine trains of five bunches spaced by 14 ns. There was no current limit imposed except through beam-beam interactions, both long-range and head-on. In this sense the optimization can and should generate an IR lattice capable of higher luminosity than can be achieved due to limitations of rf, parasitic interactions in the arcs, or beam current sensitive components. In the arcs the basic layout is more or less fixed. Separate optimizations of the IR and arc lattices may yield superior overall designs than optimizations which, for example, trade off the effects of a parasitic crossing near the IP with those of one 300 meters away.

Nevertheless, the process of separate optimization requires a means to match the two solutions without significantly degrading either. To this end I assumed constraints that require at the entrance to Q3 (a distance of about 14.5 m from the IP), $\beta_x < 30$ m, $\beta_y < 30$ m, $x_{stayclear} < 45$ mm, and the 'pretzel amplitude' $\theta\sqrt{\beta_h^*} = 2.59\ mr\ m^{1/2}$.

Variables

The parameters I most commonly used as variables are defined below. Not every optimization run varied all of them. In many cases I held several fixed, and then performed optimization on the remaining.

- I, the average beam current per beam
- $x_{Off-SR-Collision}$, the offset of the incoming beam at the IP for collision optics. This was a magnetic bump. Typical values for an optimum solution ranged between -2 and -3 mm, where the positive direction is away from the center of CESR.
- $x_{Off-SR-Injection}$, the same offset, but for injection. Again this was a magnetic bump. Though roughly in the same range as the collision SR bump it was in general a different value.
- $x_{Off-Injection}$, the offset of the positron beam at the IP due to an electrostatic bump. This generated the beam separation at the IP during injection and was typically around $0.5 - 1.0$ mm.
- β_h^*, the horizontal beta function at the IP. This is the bare lattice value, not the dynamic value. [8]
- β_v^*, the vertical beta function at the IP. Usually this was fixed at 5, 10, 15 or 20 mm but occasionally was allowed to vary. In all cases the bunch length was implicitly assumed to be less than or equal to β_v^*. Again this was the bare lattice value.
- θ, the crossing angle at the IP. The optimum ranged between 2 and 3.3 mr. To match the pretzel in the arc $\theta\sqrt{\beta_h^*}$ was held constant. This in effect meant that larger crossing angles can only be obtained with smaller β_h^*, and vice versa.
- L_{Q1}, the effective length of Q1 (which is the same as Q2). Once the RFP for the superconducting magnets was finalized, this was held fixed at 0.65 m.
- K_{pm}, the strength of the permanent magnet. This was allowed to vary but is constrained by beam and detector stayclears as well as magnetic properties of permanent magnets and mechanical interferences.
- $\phi_{Warm-Bore}$, the inside diameter of the warm bore of the cryostat. This, together with fixed assumptions about the thickness of the vacuum chamber and clearances determines the maximum physical aperture the beam sees.

Fixed Inputs

A number of inputs to the optimization program are more or less fixed in the sense that they are usually not changed even between runs. They are, in effect constraints, but I separate them from constraints below because they are less direct in their effects and are not explicitly put in as constraints in the optimizing routine.

- E the beam energy
- ϵ_{h-HEP} the horizontal emittance during collision. Usually this was taken to be 2.3×10^{-7} m, a number that Dave Rubin frequently got based of a full optimization of the entire lattice. Both wigglers were closed.
- ϵ_{h-INJ}, the same thing during injection. Usually this was 1.80×10^{-7} m, which also came from D. Rubin with both wigglers open.
- $n_{bunches}$, almost always this was 45 bunches per beam assumed to be 14 ns apart in 9 trains.
- ξ_v, the vertical tuneshift parameter. This was held fixed at 0.04 for all runs. The vertical beam size was assumed to accommodate it. While this is on the

high side, it has been obtained with crossing angles and is supposed to represent the optimum value.

- t_{vc-pm}, the radial thickness allowed for the vacuum chamber inside the permanent magnet. This includes room for cooling channels. Usually it was 6 mm.

- g_{vc-pm}, the radial gap between the outside of the vacuum chamber and the inside of the permanent magnet assembly. This is needed for installation clearance and was usually 1 mm.

- $t_{cryostat-coil}$, the radial distance between the warm bore inner radius and the superconducting coil inner radius. This space is used for the warm bore tube, an LN shield, a helium vessel and insulation. It was held fixed at 11 mm which was the dimension Tesla gave in a proposal for a prototype construction.

- g_{vc-wb} the radial gap for installation between the outside of the vacuum chamber and the inside of warm bore of the cryostat. This was 3 mm.

- $t_{vc-cryo}$ the minimum radial thickness of the vacuum chamber in the region of the cryostat. The bore here is bigger than in the permanent magnet and straightness is more important due to the length. This distance was held at 8 mm. It includes room for cooling channels.

- s_{Q1-Q2} the physical gap between the ends of the coils of Q1 and Q2 was held at 0.1 m. In general the optimization would like a smaller value, but with this constraint some room is left for mechanical linkage between the units.

The geometry of the CLEO interface was also fixed as were a number of relations between the coil size, length of curved section, position of the effective edge relative to the coil, inner radius, and location of coil within the cryostat. These were based on drawings with extrapolations for varying bore diameters. The design clearance for the cryostat to the coil ends and the physical space a coil end takes up were based on Tesla's proposal design.

Constraints

I assumed that Q1 and Q2 were identical in length to reduce overall design and construction time. This assumption tightly couples the strength requirement of Q1 with the aperture requirement of Q2. Parameters explicitly constrained are listed below:

- $\check{\rho}_{SR-Injection}$, the smallest allowed effective bend radius for the incoming beam near the center of Q2 to prevent excess SR during injection. This was determined be Stu Henderson to be about 65 m.

- $\check{\rho}_{SR-Injection}$, same thing for collision. This was 144 m which reflects the greater sensitivity when the detector is active and needs to have small deadtime.

- ξ^*_{H-LR}, the maximum horizontal long-range tune shift parameter at the IP during injection. This is controlled by the injection pretzel and was limited to 0.002.

- $\theta\sqrt{\beta^*_h}$, the product of the crossing angle at the IP with the square root of the horizontal beta function was held equal to 2.59 $mr\ mm^{1/2}$. This insures the horizontal pretzel matches, more or less to the arc.

- ξ_h the horizontal tune shift parameter at the IP was held to be less than 0.05. For a flat beam this parameter sets a limit for the maximum current per bunch which depends only on the emittance: $\xi_h \approx (r_e/2\pi\gamma)(1/\epsilon_h)$. We can approach this limit with the phase III IR design.

- $\theta_n = \theta\beta^*_y/\sigma^*_h$, the normalized crossing angle, except that β^*_y has replaced the usual σ_s. This is limited to avoid excessive beam-beam crossing angle effects. The limit was .075 and is about where we have run this past year. If this limit is exceeded one might expect a drop in ξ_v or current. Implicitly I have assumed here that $\sigma_h = \sigma_s$.

- $B_{Peak-Coil}$ the estimated peak magnetic field due to the applied gradient on the coil. This was derived from a model worked out by G. Dugan [4]. The value used to limit the design for the RFP specifications was 4.6 T. It did not included any superimposed fields. It is less than the peak field in the LEP200 magnets[6], but more than in the LEP100 magnets [5].

- $B_{collision}$ the maximum B parameter allowed for collision. The B parameter is defined assuming the CESR circumference as [7],

$$B = \frac{I_{bunch}\ [mA]}{10}\sqrt{\sum_i \left(\frac{\beta_v\ [m]\sigma_h^2\ [mm^2]}{d^2\ [mm^2]}\right)_i}$$

This is calculated from a total of the 8 long-range interactions, four on each side of the IP. It was derived from two considerations. First, machine studies experiments indicate that for good lifetime the B parameter should be less than 1. Second by comparing the total B parameter calculated for the entire ring by D. Rubin with the IR contribution, I found that the arc contributes about half of the total limit. The actual number for the limit for the IR I allowed was

0.765 which is slightly more than half of the total contribution to the ring (it adds in quadrature).

- $B_{injection}$, the maximum B parameter allowed for injection. This was limited to 1.2. somewhat arbitrarily. We don't have very good lifetime versus B parameter data. Machines studies results [10] predict a 50 minute lifetime for an average B of 1.15, with an rms of about $\pm 11\%$. With an IR limit of 1.2, if the arc contribution to B is unchanged the total for the ring would be 1.36.

- $\phi_{Warm-Bore}$, the warm bore diameter. At times it was a constraint, other times it was left to vary. Now that the specifications for the superconducting magnets are complete it will be fixed at $\phi 145$ mm.

- $\xi_{LR-Injection}$, the maximum allowed long range tune shift during injection, (excluding the IP). This was limited to 0.002 which is in the middle of the experimentally determined range for 50 minute lifetime of [.001-.003].

- ξ_{LR-HEP}, the maximum allowed long range tune shift during collision. This was limited to .001 which is the lower range of the experimentally determined range for 50 minute lifetime.

- s_{PM}, the starting position of the permanent magnet. Usually this was held fixed 0.35 m. At this value a straight bore magnet was thought to fit within the 10 cm radial allowance determined by the drift chamber ID. Actually there is some interference between such a permanent magnet and the detector cable runs and either the outer diameter will have to decrease or the starting position will have to be pushed back.

- $L_{Coil-End}$, the longitudinal length of the curved end section of the coil (one end). This length includes blocks beyond the coil for support and is based on the Tesla design, but scaled linearly with inner coil radius. A typical value was 0.13 m. The effective edge was assumed to be in the middle of the curved section.

Results

The most important parameters in the superconducting quadrupole specification are the required gradient and warm bore diameter. Magnets of this type are of necessity built close to the margin of workability — 30% theoretical current margin is considered generous. So it was with considerable care and thoroughness that I sought the optimal values.

There was a fairly clear advantage in all cases to make the quadrupoles as short and as close together as possible.

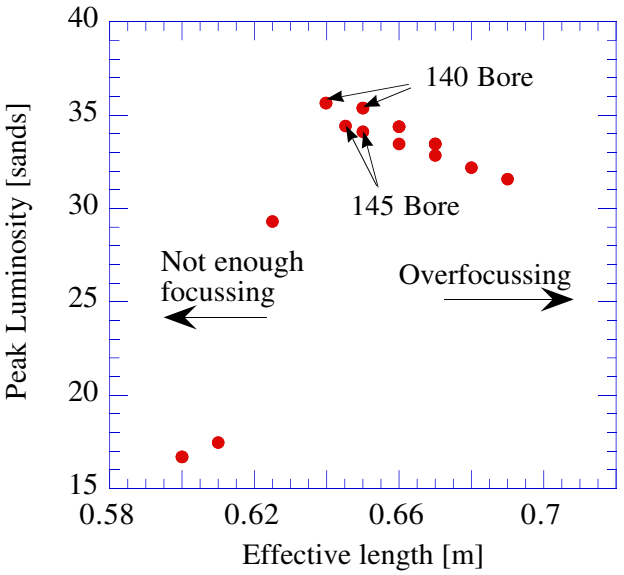

Figure 2: Optimized luminosity as a function of effective length for two different warm bore diameters is plotted. One *sands* is $10^{32}\ cm^{-2}s^{-1}$.

The shortness was only limited by the peak coil field I was willing to withstand.

Effective length

I found that if the effective length was around 0.55 m or less, the limitation of the peak coil field ruled out any solutions because the net vertical focussing was simply too weak. If the effective lengths were around 0.8 or more, the first parasitic crossing point would have a very large β_y and the current would be severly limited. Within the range of 0.60 to 0.70 m the luminosity was a fairly smooth function peaking near the shorter lengths. See figure 2.

The final choice of 0.65 m for the effective length of Q1 and Q2 represented an attempt to be near the optimum but not too close to the lower limit. It was not too clear just how accurately the thick lense hard-edge approximation that is assumed in virtually all lattice design could be expected to predict the beam performance with substantial edge effects. These interaction region quadrupoles are so short that the curved portion of the coil is about 40% of the effective length, and in Q1 the steeply rising vertical beta function is completely turned around by the point it leaves the magnet. These consideration caused me to avoid going closer to the lower effective lengths even though the luminosity there is little better.

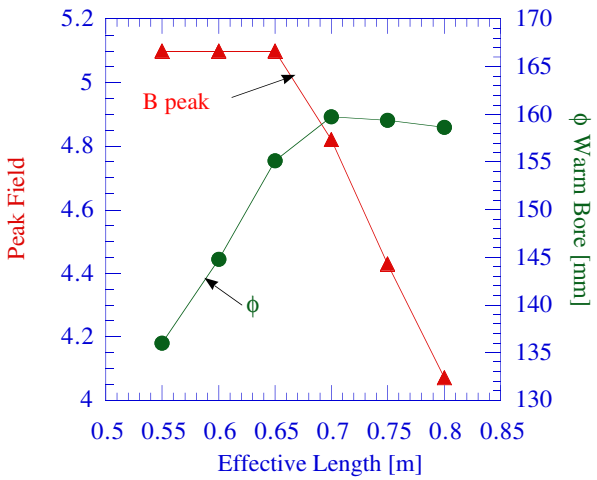

Figure 3: The peak field on the coil and the warm bore diameter are plotted for different effective lengths of the quadrupoles. The peak field is the optimized value that gives the most luminosity.

Warm bore diameter

The selection of the warm bore diameter was a rather tricky issue. The beam stayclear is determined by the horizontal size and position of the beams in Q2, at least for $\beta_y^* > 5$ mm. The maximum gradient is determined by Q1. Focussing harder vertically makes the horizontal size and offset in Q2 bigger and therefore requires a bigger bore. This was especially true for focussing by the permanent magnet since it was first. On the other hand a smaller bore diameter allowed higher gradients for the same peak field on the superconducting coil. Higher gradients allow some shortening of the quadrupoles which was beneficial. See figure 3.

I found workable solutions ranging from $\phi_{Warm-Bore}$ of 130 mm to 170 mm, with the best luminosity at the smaller diameters. Below 130 or so, there were no solutions that satisfied all the beam steering and pretzel constraints. Above 170 the luminosity dropped off rapidly as these large magnets had to start further from the IP and had lower gradients providing only weak focussing.

Another important consideration in the selection of the warm bore diameter was the required mechanical tolerance. We require 5×10^{-4} or better non-quadrupole field at 5 cm radius. If we only require the same mechanical tolerance that was obtained in the LEP200 magnets we would need to have a warm bore diameter of 140 mm or so. The required tolerance is a rather high power of the radius so a ϕ130 mm bore would be considerably harder to make.

The reduction in peak luminosity going from a bore of ϕ140 to ϕ145 was only 3%. Furthermore, the larger bore allowed a smaller β_y^* which essentially completely cancels the decrease. The opposing action of bigger bore and smaller β_y^* indicates we want some middle ground. The ϕ145 mm bore seems to be a middle ground, has high luminosity, and makes required construction tolerances quite feasible, so it was chosen for the specifications.

Permanent Magnet Effects

As mentioned above the strength of permanent magnet had a large effect in determining the required bore diameter. Stronger permanent magnets increase β_h in Q2, as well as the decrease the required strength of Q1. The net effect of the permanent magnet strength on the optimum luminosity depended rather critically on the strength of the aperture driving assumptions of offsets for synchrotron radiation and injection separation.

Early optimization runs were somewhat too conservative in requiring the incoming beam to be always on axis. These runs were also done with the assumption that the injection emittance was the same (larger value) as for collision and that the separation bump was fixed. Later runs assume the wiggler open for injection and the injection separation bump was free to vary subject to constraint only by the long-range tune shift parameter at the IP. The most significant change was a new synchrotron radiation offset criteria developed by S. Henderson, [9] appropriate for these high gradient magnets. With those changes in place the aperture was not as strongly driven and feasible solutions could be found with relatively strong permanent magnets. It is still true however, that the permanent magnet focussing reduces the available stayclear in Q2, and if made too strong will not allow any solution at any current that satisfies the stayclear conditions and the synchrotron radiation offset conditions for both injection and collision. The effect of the permanent magnet on luminosity is plotted in figure 4.

Overall performance

The IR with parameters specified in the Appendix can be expected to allow very high luminosity for a wide range of $beta_v^*$ at reasonable bunch currents. See figures 5 and 6. The peak luminosity possible, 35 sands, occurs around $\beta_y^* \approx 7.5$ mm. The peak beam current, (both total and bunch current) occurs at $\beta_v^* \approx 10$ mm. The bunch current is almost limited by the the constraint $\xi_h \leq 0.05$ and the smallness of the emittance.

In summary, with these design parameters the total current possible to inject and collide through the IR can be expected to be greater than the phase III design parameters, as it should be.

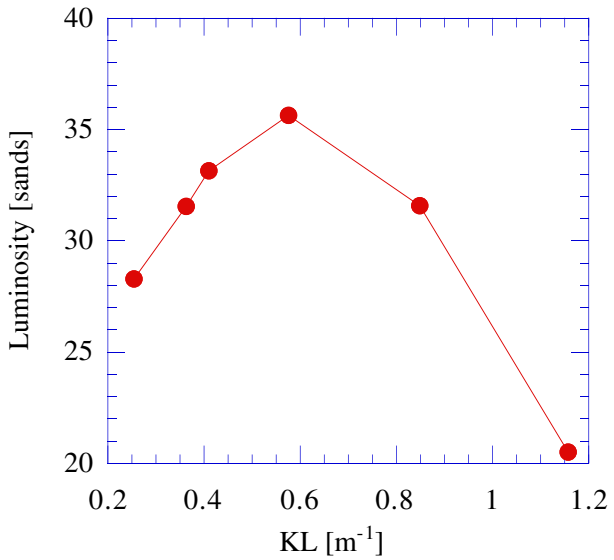

Figure 4: The effective on the IR limited optimized luminosity of the strength of the front end permanent magnet focussing.

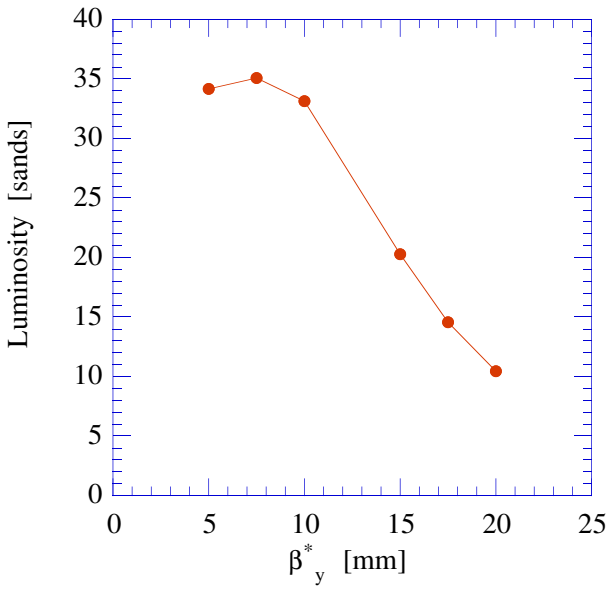

Figure 5: Optimized IR limited Luminosity as a function of β^*_y. The permanent magnet was only allowed a minimal volume. One *sands* is $10^{32}\ cm^{-2}s^{-1}$.

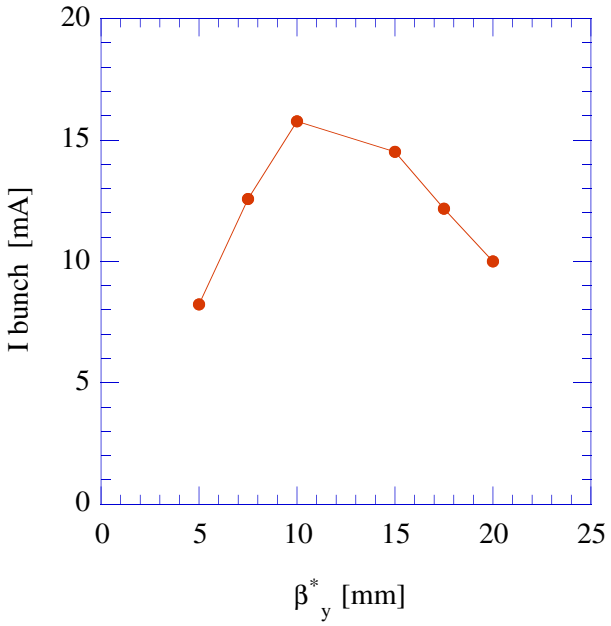

Figure 6: The maximum bunch current for IR limited luminosity as a function of β^*_h.

References

[1] Proceedings of the Workshop towards Establishing a b Factory, edited by M. Goldberg and S. Stone, Syracuse NY, September 1989.

[2] The CESR/CLEO Upgrade Project, CLNS 93/1265

[3] Talk reported in the CLEO III, Status Report, May 11-12, 1995.

[4] G. Dugan *Skew Quadrupole Windings on Q1/Q2 for the CESR Phase III IR*, CON 95-13, (1995)

[5] P. Lebrun, et. al., *Design, Test, Performance of the Prototype Superconducting Quadrupole for the LEP Low-beta Insertions* IEEE Trans on Magnetics, vol 24, no. 2, March 1988, p 1361

[6] T.M. Taylor, et. al., *Design of the Superconducting Quadrupoles for the LEP200 Low-Beta Insertions*, IEEE Trans on Magnetics, vol 28, no. 1, March 1992, p 382

[7] A. Temnykh and J.J. Welch, *Crossing Angles at CESR, Experiments and Experience*, CBN 95-13, 1995.

[8] *The Dynamic Beta Effect in CESR*, CBN 94-6, D. Sagan 1994.

[9] S. Henderson simulation based on a no permanent magnet lattice (maximal strength) circa September 1995.

[10] A.B. Temnyckh, J.J. Welch and D.H. Rice, *The Long Range Beam-Beam Interaction at CESR — Experiments, Simulation and Phenomenology*, Proc. 1993 Particle Accelerator Conf. vol 3, pg 2007.

10/19/95 10:57 AM IR Optimizer

Inputs

Title	**phase III flat, restrictive injection conditions**		
notes	*post RFP parameters*		
	length/strength of PM not completely defined yet		
Energy	5.289	GeV	
I/beam	**711**	mA	
bunches/beam	45		
betav star	**10**	mm	
betah star	0.720	m	
xi_v	0.04		
aperture drivers			
theta	**3.05**	mrad	
theta *sqrt(betah))	2.59	mr mm^1/2,	constraint on pretzel amplitude in arcs
e_h HEP	2.30E-07	m	typical minimized emittance with wigglers is 2.3e-7
e_h_inj	1.80E-07	m	emittance during injection with wigglers open
x_off SR	-2.87	mm	to reduce SR from incoming beam in Q2
x_off_sr_injection	-1.96	[mm]	SR offset during injections
x_off_inject	0.99	mm	pretzel offset for injection bump, need xi_h0 .002
min rho eff. Injection	**65**	[m]	determine by Stu H to be 11 mm for Kq2 = 1.39
min rho eff. HEP	**144**	[m]	determine by Stu H to be 5 mm for Kq2 = 1.39
xi_lr_0 max	2	[.001]	max allowed long range horzontal tune shift for injection at IP
bore drivers			
t vac ch (min) cryo	6	mm	radial gap for installation clearnance of cryostat
t_vac_pm	6	mm	radial size of vacuum chamber with cooling channels PM
gap vac pm	1	mm	radial gap between PM and vac ch for installation
t cryo inner insul	11	mm	inner radius of coil to inner radius of cryostat warm bore
gap warm bore - vac ch	3	mm	radial gap for installation clearance of cryo
t vac ch beampipe	8	mm	radial thickness of vac ch in cryo including cooling channels
l gap btw q1-q2	0.1	m	physical distance between coil ends of q1 and q2
l_eff_q12	**0.65**	m	
Q12 design warm bore ID	**145**	mm	considered input to define ri coil
magnet design limits			
B peak coil max	**4.6**	T	max allowed field on coil
Brem	1.1	T	
K PM unif. bor @5.3	**-1.6**	m^-2	for optimizing uniform bore PM
Min K PM allow @5.3	**-1.6**	m^-3	
Min r1 or PM	**33**	mm	minimum allowed inner radius of PM material
pos error of eff. edge	**0**	m	error added to longitudinal position of effective edge
long range bb limits			
B parameter limit HEP	0.765		maximum allowed total B parameter from both side of IP, HEP
B parameter limit Injectior	1.2		maximum allowed total B parameter from both side of IP, Injection
Max xi_LR HEP	0.9	[.001]	
Max xi_LR Injection	2	[.001]	

10/19/95 10:58 AM IR Optimizer

Calculated

general

Luminosity	**33.24**	"Sands 10^32"	
I/bunch	**15.8**	mA	
N	2.53E+11	particle/bunch	
max dia stay clear	**119**	[mm]	max required of injection and collision cases
xi_h	0.0468		
normalize theta	0.075	radians	should really have sigma_s instead of betay_star
sigmav star	6.72	microns	
sigmah star	407	microns	
r	1.65%		
epsilon v	4.51E-09	m	
epsilon v/epsilon h	1.96%		
IR v chromaticity	-18		
IR h chromaticity	4		

Collision Conditions

max stayclear collision	119	[mm]	
theta*sqrt*(betah)	2.59	mr mm^1/2	needed for pretzel, (2.59 dlr)
incoming pos in Q2	2.93	[mm]	should be less than 5
rho effective at Q2	**219.88**	[m]	
long range xi_v, 14ns	0.45	[0.001]	
long range xi_h, 14ns	0.56	[0.001]	
long range xi_v, 28ns	0.26	[0.001]	
long range xi_h, 28ns	0.52	[0.001]	
long range xi_v, 42ns	0.16	[0.001]	
long range xi_h, 42ns	0.46	[0.001]	
long range xi_v, 56ns	0.21	[0.001]	
long range xi_h, 56ns	0.41	[0.001]	
max LR xi	**0.56**	collision	
n sigma 14 ns pcp	6.77		
n sigma 28 ns pcp	9.24		
B parameter 14ns	0.71	inlcudes both incoming and outgoing contributions	
B parameter 28ns	0.26	ditto	
B parameter 42ns	0.08	ditto	
B parameter 56ns	0.03	ditto	
B total	**0.77**		

IR Optimizer

Injection Conditions

max stayclear injection	112	[mm]	
theta*sqrt*(betah)	2.59	mr mm^1/2	needed for pretzel, (2.59 dlr)
incoming offset Q2 e+	10	[abs mm]	
incoming offset Q2 e-	2.62	[abs mm]	
rho effective at Q2 e+	**65.40**	[m]	
rho effective at Q2 e+	**245.70**	[m]	
xi_lr_0 injection	2.00	[0.001]	IP horz. tuneshift during injection

	east	**west**	
long range xi_v, 14ns	0.28	0.85	[0.001]
long range xi_h, 14ns	0.34	1.07	[0.001]
long range xi_v, 28ns	0.17	0.44	[0.001]
long range xi_h, 28ns	0.34	0.88	[0.001]
long range xi_v, 42ns	0.12	0.23	[0.001]
long range xi_h, 42ns	0.34	0.64	[0.001]
long range xi_v, 56ns	0.22	0.20	[0.001]
long range xi_h, 56ns	0.43	0.39	[0.001]
max LR xi	**0.43**	**1.07**	
B parameter 14ns	0.31	0.96	inlcudes both incoming and outgoing contributions
B parameter 28ns	0.12	0.32	ditto
B parameter 42ns	0.04	0.07	ditto
B parameter 56ns	0.02	0.02	ditto
B total per side	**0.34**	**1.01**	
B Total	**1.07**		

Magnet Parameters

l_physical q12	0.81	m	
ri coil (min)	87.57	mm	limited by beam stayclear
ri coil design	89.50		
l_coil_design	0.161597	m	length of curved part of coil
r_corner_collar design	163.80	mm	radially outer position of the innermost part of the collar
zp design	761.34	mm	physical position of the edge of the coil closest to the IP
s_q1 design	0.842143	m	
vac ch OD (min)	135.14	mm	5.32 inches
vac ch ID (min)	119.14	mm	4.69 inches
min ID warm bore	**141.14**		
des ID warm bore	**145.00**		
B_peak coil (min)	4.60	T	scaled from Dugan skew quad paper assuming min bore
Q1 gradient	-43.96	T/m	
Q2 gradient	27.38	T/m	
s_cryo_front	0.585		

Lattice Calculation

	S	K	L	B pole	dB/dr	Ri	Ro	beta h at ei	beta v at end	Chrom	Chrom	Q_H [rad/2 PI]	Q_V [rad/2 PI]
	0	*0*	*0*	*T*	*T/m*	*mm*	*mm*	of element *0.72007*	of element *0.01*	*vert*	*vert*	MOD(1) *0.00*	MOD(1) *0.00*
dont kill this row	0.35	0.00	0.35					**0.89**	**12.26**	0.00	0.00	0.07	0.25
	0.59	-1.7096	0.24	0.94	30	31	62	**1.30**	**31.96**	-2.05	-0.08	0.11	0.25
-5.29979E-05	0.59	0.00	0.00	0.94	0	#####	######	**1.30**	**31.97**	-2.05	-0.08	0.11	0.25
	0.59	0.00	0.00	0.94	0	#####	######	**1.30**	**31.98**	-2.05	-0.08	0.11	0.25
	0.59	0.00	0.00	0.94	0	#####	######	**1.30**	**31.99**	-2.05	-0.08	0.11	0.25
	0.59	0.00	0.00	0.94	0	#####	######	**1.30**	**32.00**	-2.05	-0.08	0.11	0.25
	0.59	0.00	0.00	0.94	0	#####	######	**1.30**	**32.01**	-2.05	-0.08	0.11	0.25
	0.59	0.00	0.00					**1.30**	**32.01**	-2.05	-0.08	0.11	0.25
Q1 starts here	0.842143	0.00	0.26					**2.11**	**59.97**	-2.05	-0.08	0.13	0.25
	1.17	**-2.49**	**0.33**		-44	T/m		**4.38**	**86.10**	-13.14	-0.65	0.15	0.25
	1.49	**-2.49**	**0.33**		-44	T/m		**10.95**	**70.98**	-22.29	-2.06	0.16	0.25
Q2 starts here	1.75	0.00	0.26					**21.08**	**46.16**	-22.29	-2.06	0.16	0.25
parasitic point 2.1	**2.10**	**1.55**	**0.35**		**27**	**T/m**		**33.85**	**27.15**	**-19.97**	**0.84**	**0.16**	**0.25**
	2.25	**1.55**	**0.15**		27	**T/m**		**36.32**	**23.40**	-19.09	2.20	0.16	0.25
	2.40	**1.55**	**0.15**		27	**T/m**		**36.24**	**21.51**	-18.29	3.56	0.16	0.25
parasitic point 4.2	**4.20**	**0.00**	**1.80**					**21.83**	**10.86**	**-18.29**	**3.56**	**0.17**	**0.27**
	5.20	0.00	1.00					**15.49**	**6.68**	-18.29	3.56	0.18	0.29
parasitic point 6.3	**6.30**	**0.00**	**1.10**					**9.89**	**3.52**	**-18.29**	**3.56**	**0.20**	**0.33**
	7.30	0.00	1.00					**6.05**	**1.96**	-18.29	3.56	0.22	0.39
parasitic point 8.4	**8.40**	**0.00**	**1.10**					**3.22**	**1.68**	**-18.29**	**3.56**	**0.26**	**0.49**
	14.58	0.00	6.18					**14.17**	**28.18**	-18.29	3.56	0.43	*0.83*
Q3 VF	15.18	-0.30	0.60					**19.51**	**30.00**	-19.15	3.00	0.42	*0.83*

IR Optimizer

Colliding Conditions												
sigma_h [mm]	12 sig_cpld [mm]	12 sig_h [mm]	X_CO [mm] incoming	X_CO [mm] outgoing	beam separation [mm]	v_aperture [mm]	h_aperture [mm]	radial stay clear [mm]	long range xi v, [.001]	long range xi h, [.001]	beam separation no. sigma-h	B parameter
						38.76	**59.57**	**59.57**				
0.41	0.41	4.88	-2.8668	-2.8668	0.00	1.41	8.75	8.75			0.00	
0.45	14.25	5.43	-1.80	-3.94	2.14	15.25	10.36	15.25			4.72	
0.55	23.01	6.56	-1.15	-4.85	3.70	24.01	12.41	24.01			6.76	
0.55	23.01	6.56	-1.15	-4.85	3.70	24.01	12.42	24.01			6.76	
0.55	23.01	6.56	-1.15	-4.85	3.70	24.01	12.42	24.01			6.76	
0.55	23.02	6.56	-1.15	-4.85	3.70	24.02	12.42	24.02			6.76	
0.55	23.02	6.56	-1.15	-4.85	3.70	24.02	12.42	24.02			6.77	
0.55	23.02	6.57	-1.15	-4.86	3.70	24.02	12.42	24.02			6.77	
0.55	23.03	6.57	-1.15	-4.86	3.70	24.03	12.42	24.03			6.77	
0.70	31.51	8.36	-0.52	-6.09	5.56	32.51	15.45	32.51			7.99	
1.00	37.76	12.04	0.24	-8.54	8.78	38.76	21.58	38.76			8.75	
1.59	34.28	19.04	1.07	-13.28	14.36	35.28	33.33	35.28			9.05	
2.20	27.65	26.43	1.83	-18.32	20.15	28.65	45.75	45.75			9.15	
2.79	**21.20**	**33.48**	**2.62**	**-23.10**	**25.73**	**22.20**	**57.59**	**57.59**	**0.45**	**0.56**	**9.22**	**0.71**
2.89	19.68	34.68	2.83	-23.89	26.72	20.68	59.57	59.57			9.24	
2.89	18.87	34.64	2.93	-23.82	26.75	19.87	59.47	59.47			9.27	
2.24	**13.41**	**26.89**	**3.53**	**-17.99**	**21.52**	**14.41**	**45.88**	**45.88**	**0.26**	**0.52**	**9.60**	**0.26**
1.89	10.52	22.65	3.87	-14.74	18.60	11.52	38.39	38.39			9.86	
1.51	**7.63**	**18.10**	**4.24**	**-11.16**	**15.40**	**8.63**	**30.26**	**30.26**	**0.16**	**0.46**	**10.21**	**0.08**
1.18	5.69	14.16	4.57	-7.91	12.48	6.69	23.07	23.07			10.58	
0.86	**5.27**	**10.32**	**4.94**	**-4.34**	**9.28**	**6.27**	**16.26**	**16.26**	**0.21**	**0.41**	**10.79**	**0.03**
1.81	21.60	21.67	15.74	7.01	8.73	22.60	38.41	38.41			4.84	
2.12	22.29	25.42	18.58	7.59	10.99	23.29	45.00	45.00			5.19	

Injection Conditions																			
		e+		e-		Separation		v_aperture	h_aperture	radial stay	xi_v		xi_h		n_sigma		B	
12 sig_cpl [mm]	12 sig_h [mm]	X_CO in	X_CO out	X_CO in	X_CO out	east [mm]	west [mm]	[mm] **34.40**	[mm] **55.88**	clear [mm] **55.88**	east	west	east	west	east **4.88**	west **4.88**	parameters east	west
0.36	4.32	-0.97	-0.97	-2.95	-2.95	1.98	1.98	1.36	8.27	8.27	0.03	0.03	2.00	2.00	4.88	4.88	**0.00**	**0.00**
12.61	4.80	0.10	-2.04	-1.88	-4.02	4.12	0.15	13.61	9.82	13.61								
20.35	5.81	0.84	-2.86	-1.24	-4.94	5.78	1.62	21.35	11.75	21.35								
20.35	5.81	0.84	-2.86	-1.24	-4.94	5.78	1.62	21.35	11.75	21.35								
20.36	5.81	0.84	-2.86	-1.24	-4.94	5.78	1.62	21.36	11.75	21.36								
20.36	5.81	0.84	-2.86	-1.24	-4.94	5.78	1.62	21.36	11.75	21.36								
20.36	5.81	0.84	-2.86	-1.24	-4.94	5.78	1.62	21.36	11.75	21.36								
20.37	5.81	0.84	-2.86	-1.24	-4.94	5.78	1.62	21.37	11.75	21.37								
20.37	5.81	0.84	-2.86	-1.24	-4.94	5.78	1.62	21.37	11.75	21.37								
27.88	7.40	1.67	-3.90	-0.62	-6.18	7.85	3.28	28.88	14.58	28.88								
33.40	10.66	2.99	-5.79	0.12	-8.66	11.65	5.91	34.40	20.31	34.40								
30.33	16.85	5.12	-9.24	0.89	-13.46	18.58	10.13	31.33	31.31	31.33								
24.46	23.38	7.29	-12.86	1.58	-18.56	25.85	14.44	25.46	42.94	42.94								
18.76	**29.62**	**9.41**	**-16.32**	**2.32**	**-23.40**	**32.81**	**18.64**	**19.76**	**54.02**	**54.02**	**0.28**	**0.85**	**0.34**	**1.07**	**11.76**	**6.68**	**0.31**	**0.96**
17.41	30.68	9.81	-16.91	2.52	-24.20	34.01	19.43	18.41	55.88	55.88								
16.69	30.65	**9.85**	-16.90	**2.62**	-24.13	33.98	19.52	17.69	55.78	55.78								
11.86	**23.79**	**8.32**	**-13.20**	**3.32**	**-18.20**	**26.52**	**16.52**	**12.86**	**42.99**	**42.99**	**0.17**	**0.44**	**0.34**	**0.88**	**11.83**	**7.37**	**0.12**	**0.32**
9.30	20.04	7.47	-11.14	3.71	-14.90	22.37	14.84	10.30	35.93	35.93								
6.75	**16.01**	**6.53**	**-8.87**	**4.13**	**-11.27**	**17.80**	**13.00**	**7.75**	**28.28**	**28.28**	**0.12**	**0.23**	**0.34**	**0.64**	**11.80**	**8.62**	**0.04**	**0.07**
5.04	12.53	5.68	-6.81	4.52	-7.96	13.64	11.33	6.04	21.49	21.49								
4.66	**9.13**	**4.74**	**-4.54**	**4.95**	**-4.33**	**9.07**	**9.49**	**5.66**	**15.08**	**15.08**	**0.22**	**0.20**	**0.43**	**0.39**	**10.55**	**11.03**	**0.02**	**0.02**
19.11	19.17	8.20	-0.53	16.07	7.34	0.86	16.60	20.11	36.24	36.24								
19.72	22.49	9.91	-1.08	18.97	7.98	1.93	20.04	20.72	42.45	42.45								